Expanded View Figures

Figure EV1. BT308FO and BT275FO GSCs: Omomyc inhibits cell proliferation, migration and self-renewal, but promotes differentiation.

A Proliferation plot of BT308FO (left) and BT275FO (right), measured by proliferative kinetic analysis upon Dox treatment, 0–96 h. Viable cells were counted using a haemocytometer.

B Percentage of cells that were capable of forming new secondary neurospheres after 7 days in the presence or absence of Dox.

C Transwell migration assay of BT275FO and BT308FO cells after 3 days with or without Dox. 10 fields were counted per assay.

D qRT–PCR of relevant markers *CCND1* (cyclin D1), *SOX2*, *NOTCH1*, *NESTIN* and *PTEN* in BT275FO and BT308FO after 48 h of induction with Dox compared to uninduced cells. *PTEN* was analysed only in BT275FO since it is not expressed in BT308FO cells. For each cell line, the expression level of each gene in non-induced cells was set as 1, and relative expression was calculated by normalizing to GAPDH.

E Immunofluorescence images representative of three independent experiments, in which BT275FO and BT308FO cells grown for 2–7 days in differentiation conditions were fixed and analysed for the presence of βIII-tubulin, GFAP and NESTIN markers. Nuclei were identified by DAPI staining and the expression of Omomyc in doxycycline-induced cells was revealed by FLAG staining (insets). Scale bars = 100 μm.

Data information: Data in panels (A–D) represent means ± SD from three independent experiments performed in triplicate.

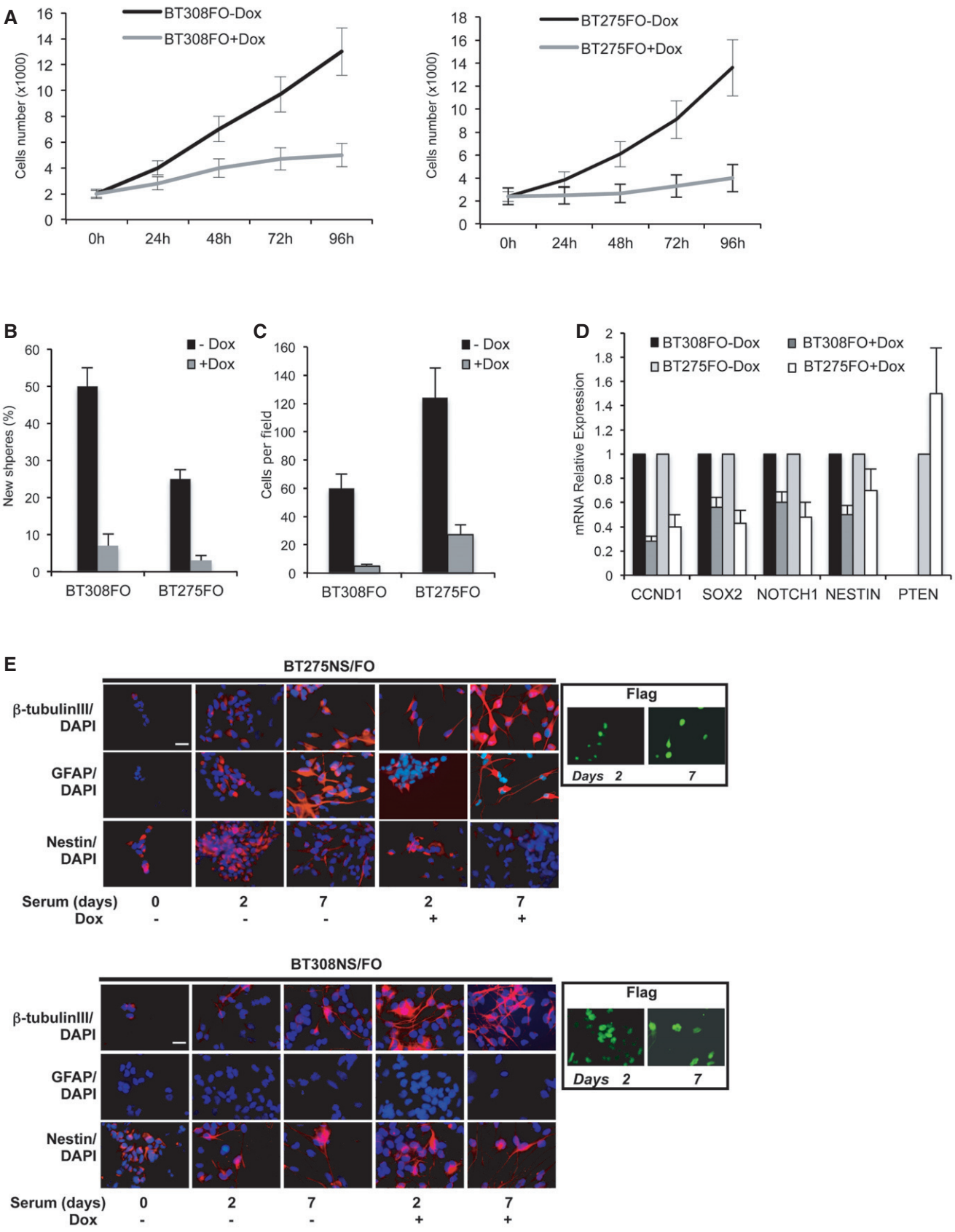

Figure EV1.

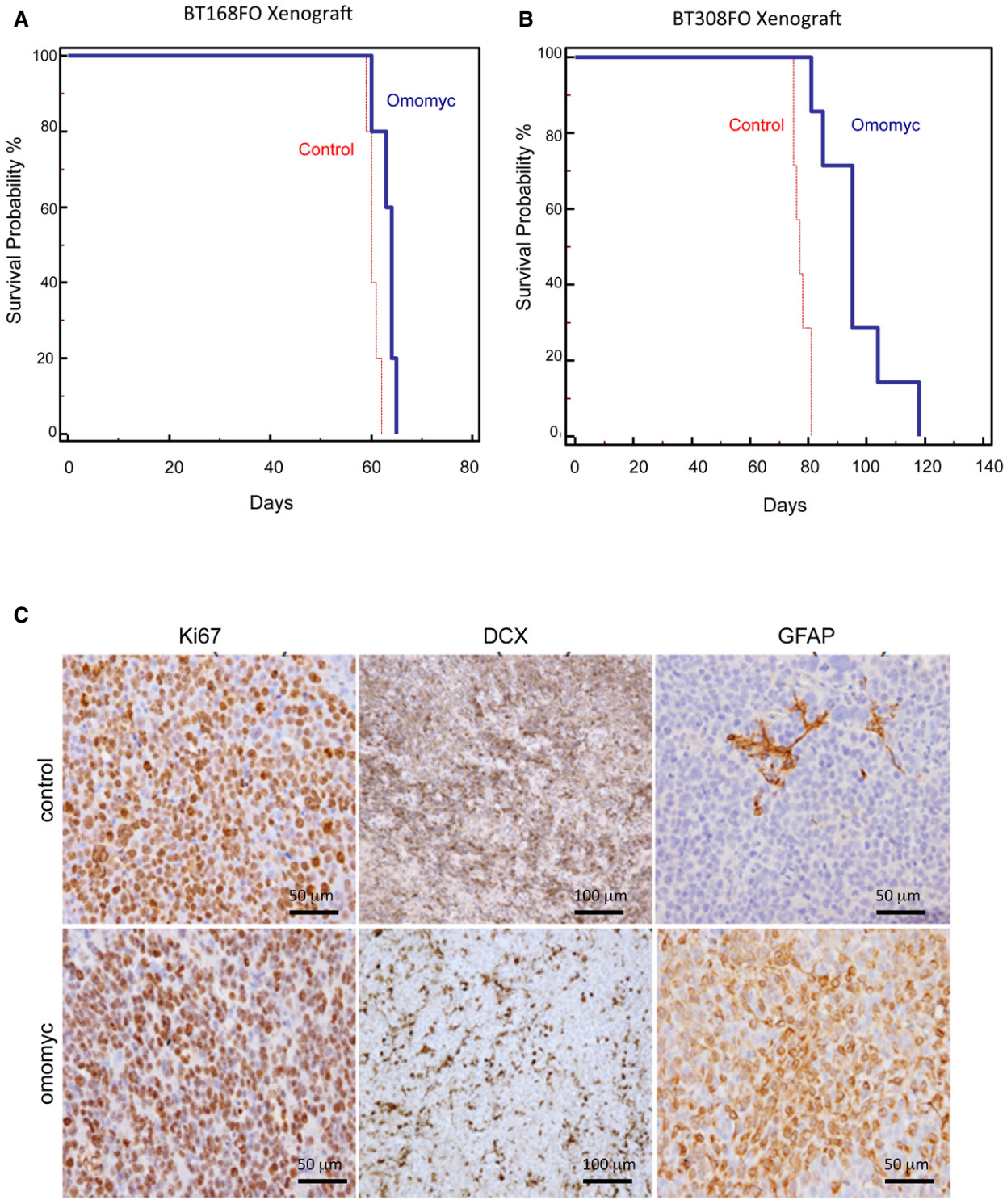

Figure EV2. Omomyc expression in BT168 and BT308 GSC xenografts results in improved survival and decreased aggressiveness.

A, B Cumulative survival curves constructed according to the Kaplan–Meier method show an increased survival of mice after implantation of Omomyc-expressing GSCs compared to controls (n = 7/group/cell line; P = 0.01 for BT168; P = 0.0006 for BT308).

C Immunostaining of Ki67, DCX and GFAP on BT308 xenograft tumours derived from control and Omomyc-expressing GSCs (n = 3/group/cell line).

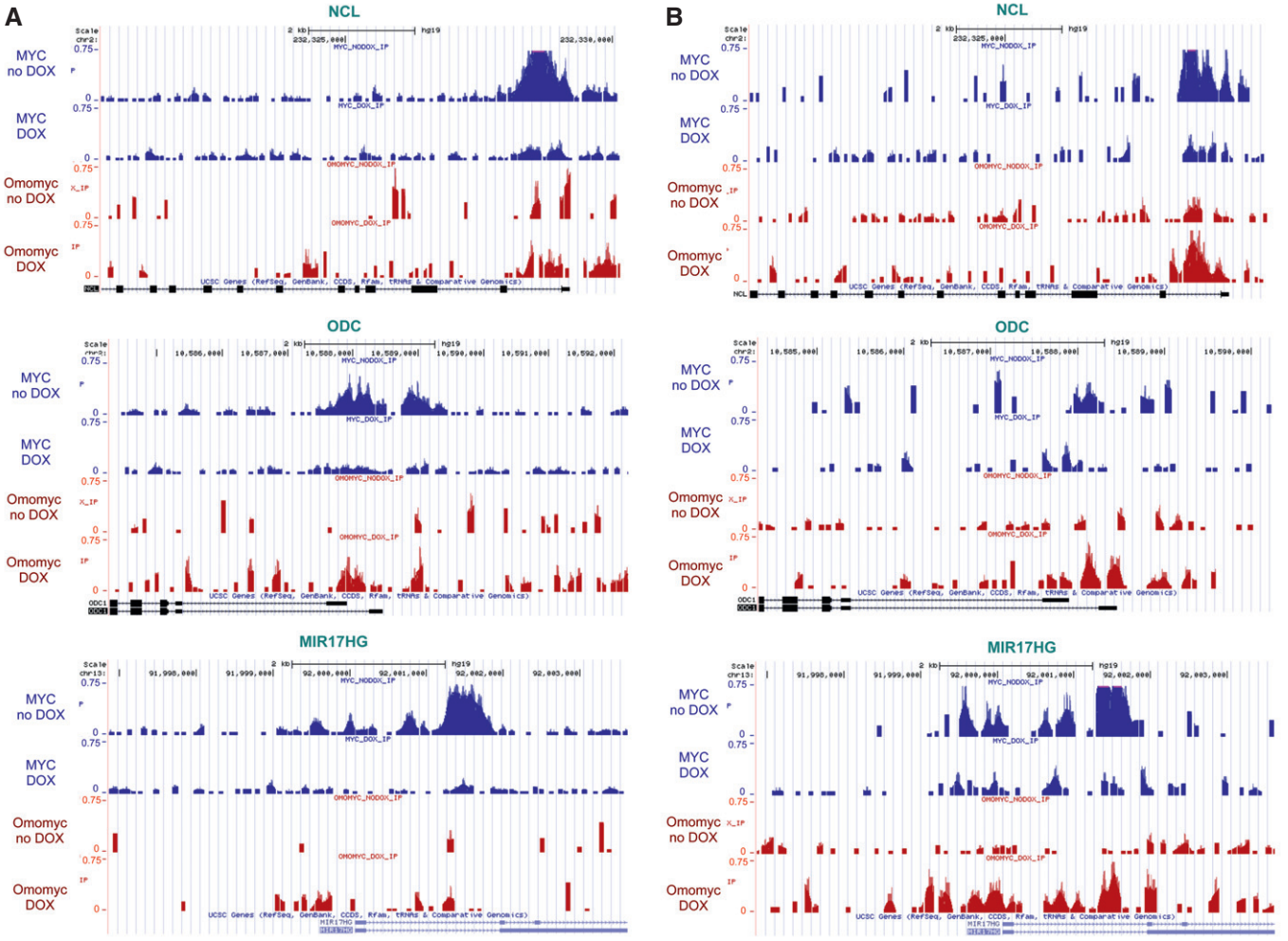

Figure EV3. MYC and Omomyc ChIP-seq signals at select target genes.

A, B Tracks of MYC (blue) and FlagOmomyc (red) binding enrichments at three select MYC target genes: *NCL* (nucleolin), *MIR17HG* (host gene of the miR-17-92 microRNA cluster), and *ODC1* (ornithine decarboxylase) in BT168FO (A) and U87FO (B) cells treated or not with Dox. The *x*-axis displays genomic position. The *y*-axis shows normalized signal intensities in RPM (reads per million).

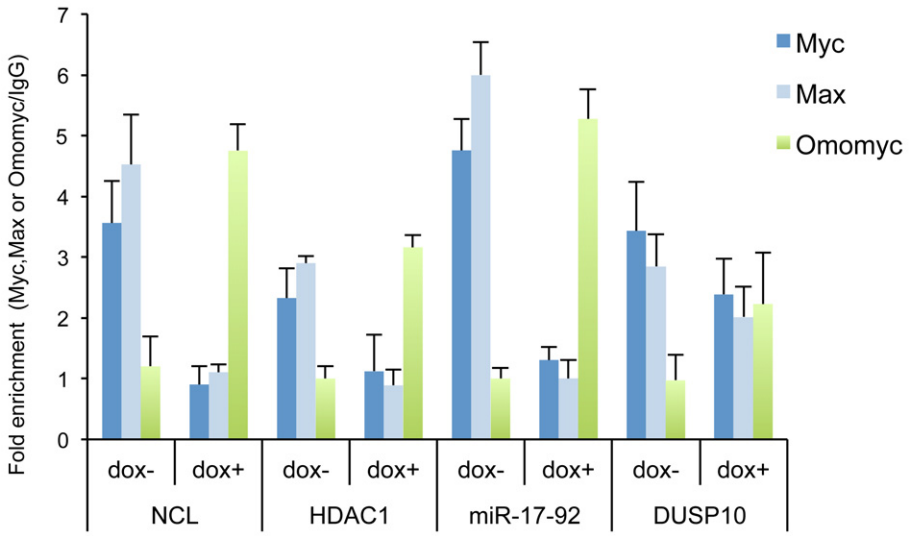

Figure EV4. Attenuation of MYC and MAX binding and concomitant Omomyc binding at *NCL*, *miR-17-92*, *HDAC1* and *DUSP10* promoters.
ChIP assay of chromatin isolated from BT168FO cells treated or not with Dox and immunoprecipitated by Flag, Myc, Max antibodies and control IgGs. qPCR analysis of immunoprecipitated chromatin was done with primers targeted to *NCL* (*nucleolin*), *miR-17-92*, *HDAC1* and *DUSP10* promoters ($n = 3$; mean ± SEM). The data show occupancy relative to control IgG.

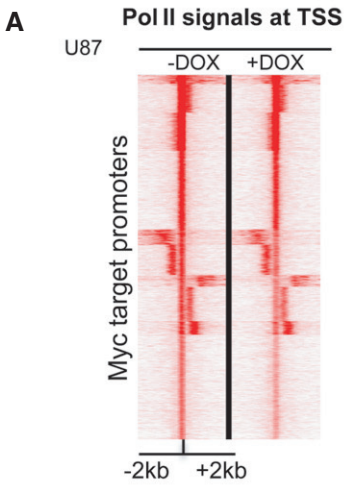

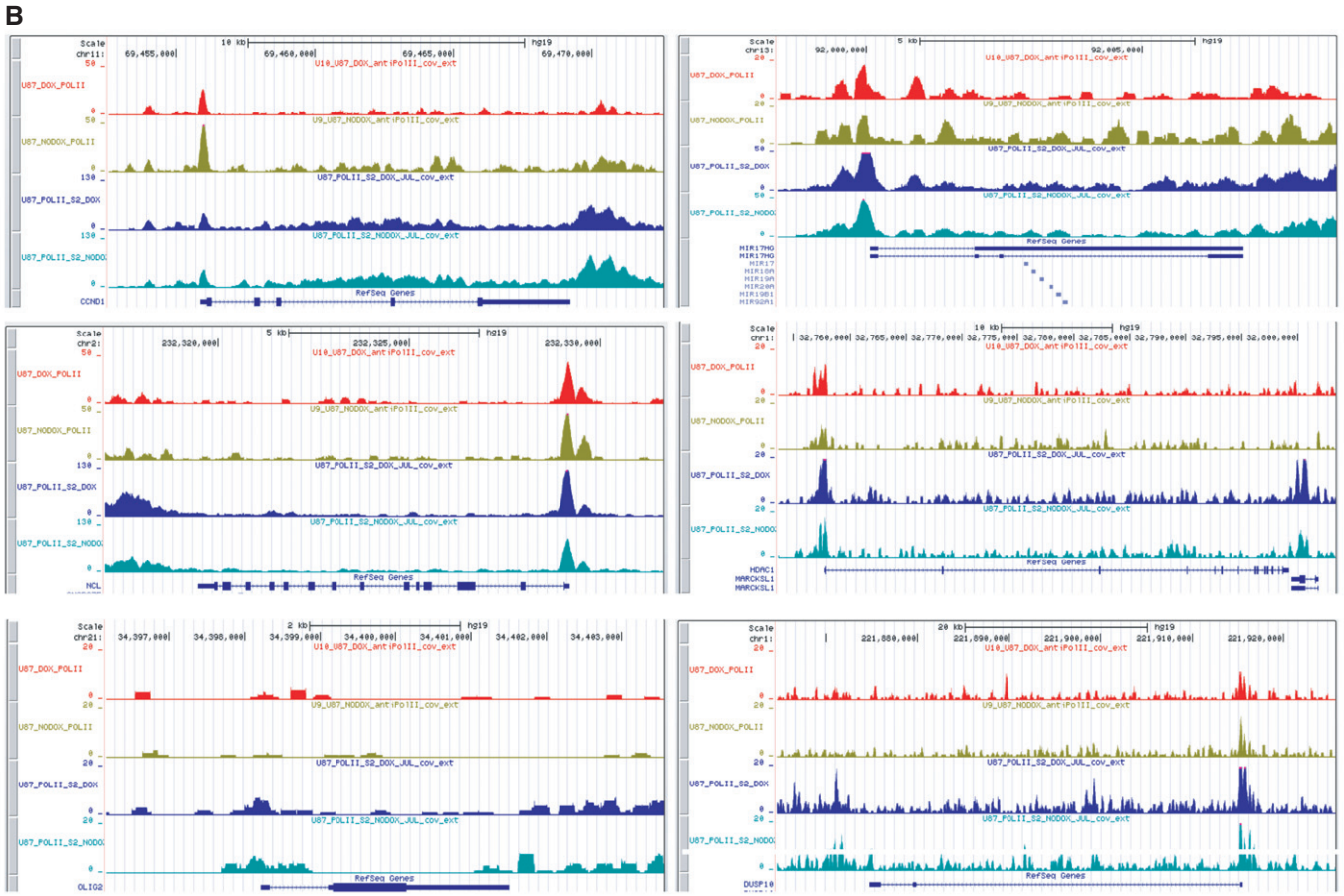

Figure EV5. RNA Pol II and Pol II Ser2p loading is minimally affected by Omomyc.

A Seqminer heatmaps of Pol II levels around TSSs of MYC promoter-target genes in U87FO cells, treated or not with Dox for 24 h. Each row shows the ± 2 kb regions centred on TSSs. Colour scaled intensities are in tags/50 bp.

B Gene tracks of RNA Pol II (top two tracks for each gene) and Pol II Ser2p (bottom two tracks) binding at *CCND1*, *NCL*, *OLIG2*, *MIR17HG (miR-17-92)*, *HDAC1* and *DUSP10* genes in U87FO cells treated (DOX) or untreated (NODOX) with Dox for 24 h.